arXiv:astro-ph/9603103v1 19 Mar 1996

WFPC2 OBSERVATIONS OF STAR CLUSTERS IN THE MAGELLANIC CLOUDS: I. THE LMC GLOBULAR CLUSTER HODGE 11[1]

KENNETH J. MIGHELL AND R. MICHAEL RICH[2]

Dept. of Astronomy, Columbia University 538 W. 120th Street, New York, NY 10027
Electronic mail: mighell@figaro.phys.columbia.edu, rmr@carmen.phys.columbia.edu

MICHAEL SHARA AND S. MICHAEL FALL

Space Telescope Science Institute, 3700 San Martin Drive, Baltimore, MD 21218
Electronic mail: mshara@stsci.edu, fall@stsci.edu

ABSTRACT

We present our analysis of *Hubble Space Telescope* Wide Field Planetary Camera 2 observations in F555W (broadband V) and F450W (broadband B) of the globular cluster Hodge 11 in the Large Magellanic Cloud galaxy. The resulting V vs. $B - V$ color-magnitude diagram reaches 2.4 mag below the main-sequence turnoff (which is at $V_{\mathrm{TO}} = 22.65 \pm 0.10$ mag or $M_V^{\mathrm{TO}} = 4.00 \pm 0.16$ mag). Comparing the fiducial sequence of Hodge 11 with that of the Galactic globular cluster M92, we conclude that, within the accuracy of our photometry, the age of Hodge 11 is identical to that of M92 with a relative age-difference uncertainty ranging from 10% to 21%. Provided that Hodge 11 has always been a part of the Large Magellanic Cloud and was not stripped from the halo of the Milky Way or absorbed from a cannibalized dwarf spheroidal galaxy, then the oldest stars in the Large Magellanic Clouds and the Milky Way appear to have the same age.

---

1. INTRODUCTION

The oldest stars for which reliable ages can be determined are found in globular clusters. Of the various methods used to infer ages in these systems, the absolute magnitude of the main-sequence turnoff is considered to be the most secure measurement. The main-sequence turnoff point for old stars occurs at $M_V \approx +4.0$ mag which makes it difficult to observe the old turnoff population in relatively nearby galaxies such as Andromeda (M31) even with the refurbished *Hubble Space Telescope*. The ages of the oldest stars in a cluster of galaxies can be used to establish the chronology of galaxy formation within that cluster. The age-spread of the oldest stars provides an important cosmological probe for the investigation of synchronized galaxy formation. Current technology, unfortunately, allows us to conduct this experiment only with the Milky Way and its relatively nearby companions.

Efforts have been made to infer the ages of star clusters in the Magellanic Clouds from their integrated photometry. The Large Magellanic Cloud (LMC) star cluster Hodge 11 (Hodge 1960) was classified by Searle, Wilkinson, & Bagnuolo (1980) as being SWB class VII and suggested that Hodge 11 is similar to the old metal-poor Galactic halo globular clusters. This was confirmed by Elson & Fall (1988) and Girardi *et al.* (1995) whose new UBV cluster photometry places Hodge 11 clearly among the oldest Galactic globular clusters. The LMC globular cluster NGC 2257 was recently thought to be similar to Hodge 11, however Testa *et al.* (1995) has determined that NGC 2257 is 2–3 Gyr younger than the oldest Galactic globular clusters. Therefore, Hodge 11 is especially interesting because it might be the oldest globular cluster in the Magellanic Clouds.

This paper presents the first results of our *Hubble Space Telescope* snapshot observation program of star clusters in the Magellanic Clouds using the Wide Field Planetary Camera 2 instrument. Our sample of star clusters was chosen to cover the full age range available in the Clouds and we have surveyed 46 star clusters using ∼15 hours of spacecraft time. While the principal aim of our observational program was to investigate the global properties of star clusters in the Magellanic Clouds, we now turn to our results on the Large Magellanic Cloud globular cluster Hodge 11.

2. OBSERVATIONS AND PHOTOMETRIC REDUCTIONS

The LMC globular cluster Hodge 11 was observed with the *Hubble Space Telescope* Wide Field Planetary Camera 2 (WFPC2) on 1994 February 1 through the F450W (broadband B) and F555W (broadband V) filters. The WFPC2 has four internal cameras

— the Planetary Camera (PC) with a focal ratio of $f/28.3$ and three Wide Field (WF) Cameras at $f/12.9$ (Holtzman *et al.* 1995a). Each camera images onto a Loral 800×800 CCD which gives a plate scale of $0\rlap{.}''046$ pixel^{-1} for the PC camera and $0\rlap{.}''10$ pixel^{-1} for the three WF cameras. The WFPC2 PC1 aperture (Burrows 1994) was centered on the target position of $\alpha = 06^{\mathrm{h}}\ 14^{\mathrm{m}}\ 23^{\mathrm{s}}$ and $\delta = -69°\ 50'\ 50''$ (J2000.0) and two high-gain observations were obtained: 600-s in F450W and 300-s in F555W. The two datasets (F450W: U26M0F01T; F555W: U26M0F02T) were recalibrated using the `calwp2` task in the `stsdas.hst_calib.wfpc` package (`IRAF V2.10.3BETA` and `STSDAS Version 10.3.2`) and the calibrated reference files are given in Table 1. All pixels that were flagged "bad" in the data quality files of the original observations were replaced by linearly interpolated values of nearby "good" pixels by using the `wfixup` task.

Unsharp masks of the Hodge 11 observations were made using the LPD (low-pass difference) digital filter which was designed by Mighell to optimize the detection of faint stars in *HST* WF/PC and WFPC2 images (Appendix A of Mighell & Rich 1995, and references therein). The two unsharp mask images were then added together to make a master unsharp mask image for each WFPC2 CCD. A simple peak detector algorithm was then used on the master unsharp images to create a list of point source candidates with coordinates $60 \le x \le 790$ and $60 \le y \le 790$ on each CCD. This allowed us to use almost the entire field-of-view of each WFPC2 camera while avoiding edge-effects in the outer regions.

We analyzed the data with the `CCDCAP` digital circular aperture photometry code recently developed by Mighell to analyze *HST* WF/PC and WFPC2 observations (Mighell & Rich 1995, 1996, and Rich & Mighell 1995). A fixed aperture with a radius of 1.8 pixels was used for all stars on the PC and WF CCDs. The local background level was determined from a robust estimate of the mean intensity value of all pixels between 1.8 and 4.8 pixels from the center of the circular stellar aperture. Point source candidates were rejected if either one of two criteria was satisfied: (1) the measured signal-to-noise ratio $SNR < 5$; or (2) the center of the aperture (which we allowed to move in order to maximize the SNR) changed by more than 2 pixels from its detected position on the master unsharp mask. These criteria allowed us to automatically eliminate most of the photon noise spikes due to the background sky and diffraction spikes. For comparison, we also reduced the data using the `DAOPHOT` program (Stetson 1987) and found that photometric scatter was significantly larger in the `DAOPHOT` photometry than in the `CCDCAP` photometry.

These observations were obtained when the WFPC2 CCDs operated at a temperature -76 °C. At this temperature, the number of "hot" pixels on a WFPC2 CCD would grow at a rate of several thousand pixels per month per chip (Holtzman *et al.* 1995a). There was

a small but statistically significant position shift for stars between the F450W and F555W frames. Hot pixels and other CCD defects did not exhibit this position shift. We took advantage of this fact to reject all point-source candidates with a position shift between the two frames that was not within five standard deviations of the mean shift on each WFPC2 CCD. This procedure allowed us to easily remove almost all of the hot pixels and other CCD defects.

Observed WFPC2 point spread functions (PSFs) vary significantly with wavelength, field position, and time (Holtzman *et al.* 1995a). There were not enough bright isolated stars in our Hodge 11 observations to allow us to adequately measure the variation of the point spread function across the WFPC2 CCDs using the observations themselves. We have determined aperture corrections (Δm_r) based on measurements of artificial point spread functions synthesized by the `Tiny Tim Version 4.0b` software package (Krist 1993, 1994). We created a catalog of 289 synthetic M-giant point spread functions in a 17×17 square grid for each filter (F450W and F555W) and CCD (PC1, WF2, WF3, and WF4). The spatial resolution of one synthetic PSF every 50 pixels in x and y allowed us to determine aperture corrections for any star in the entire WFPC2 field-of-view to within a worst-case spatial resolution of 35 pixels. The average aperture corrections ($\overline{\Delta m_r}$) are listed in Table 2.

The WFPC2 point spread functions can vary with time due to spacecraft jitter during exposures and small focus changes caused by the *HST* expanding and contracting ("breathing") once every orbit. These temporal variations of WFPC2 PSFs can cause small, but significant, systematic offsets in the photometric zeropoints when small apertures are used. Fortunately, these systematic offsets can be easily calibrated away by simply measuring bright isolated stars on each CCD twice: once with the small aperture and again with a larger aperture. The robust mean magnitude difference between the large and small apertures is then zero-order aperture correction (Δm_0) for that particular CCD and filter combination (see Table 2). On the PC1 CCD, we used a large aperture with a radius of 5.0 pixels and the background was determined using an annulus of $5.0 \leq r_{\mathrm{sky}} \leq 13.0$ pixels. On the WF CCDs, we used a large aperture with a radius of 3.0 pixels and the background was determined using an annulus of $3.0 \leq r_{\mathrm{sky}} \leq 6.0$ pixels. These large apertures contain about 86% of the total flux from a star.

We use the standard WFPC2 color system (Holtzman *et al.* 1995b) which is defined using apertures $1''$ in diameter that contain about 90 percent of the total flux from a star. A final aperture correction (Δm_∞) was added to the instrumental magnitudes to go from an infinite aperture to an aperture $1''$ in diameter (see Table 2). The Charge Transfer Effect was then removed using a uniform wedge along the Y-axis of each chip as described in

Holtzman *et al.* (1995b). Finally, the instrumental magnitudes, b and v, were transformed to Johnson B and V using the following color equations

$$
\begin{aligned}
B \;=\; & b + [0.230 \pm 0.006](B-V) \\
& + [-0.003 \pm 0.006](B-V)^2 \\
& + [21.175 \pm 0.002]
\end{aligned}
\tag{1}
$$

(Table 10 of Holtzman *et al.* 1995b) and

$$
\begin{aligned}
V \;=\; & v + [-0.060 \pm 0.006](B-V) \\
& + [0.033 \pm 0.002](B-V)^2 \\
& + [21.725 \pm 0.004]
\end{aligned}
\tag{2}
$$

(Table 7 of Holtzman *et al.* 1995b) where an instrumental magnitude of zero is defined as one DN/sec at the high gain state ($\sim$14 e$^-$/DN).

3. THE COLOR-MAGNITUDE DIAGRAM OF HODGE 11

The early photographic photometry of Gascoigne (1966) clearly revealed the unusual nature of Hodge 11: its large number of very blue stars and the absence of a defined giant branch. While some electronographic photometry of Hodge 11 was attempted, little substantive progress occurred until the CCD photometry of Stryker *et al.* (1984), which clearly identified the blue horizontal branch and M92-like red giant branch after a careful subtraction of the substantial contaminating LMC field population. Walker's (1993) study represents the best ground-based photometry of Hodge 11 to date but his field-subtracted color-magnitude diagram only reaches $V \approx 22$ mag which is $\sim$3 mag below the horizontal branch and $\sim$0.5 mag above the main-sequence turnoff of an old ($\sim$15 Gyr) globular cluster. We have compared our photometry of giants in Hodge 11 with the data set of Alistair Walker (1993) which he kindly provided to us. Using only the WF4 CCD, we find 80 giants in common between the two data sets. Figure 1 shows that there is a statistically insignificant difference between the V zeropoints of the two data sets (0.009 ± 0.010 mag with our V photometry being $\sim$1% fainter).

The V vs $B-V$ color-magnitude diagram (CMD) of our observed stellar field in Hodge 11 reaches $V \approx 25.0$ mag and is displayed in Fig. 2. Figure 2a shows all the data with 13175 stars (filled circles) and 1855 CCD defects (open circles). Hodge 11 is surrounded by a field population that is mostly 2–3 Gyr old with a metallicity of [Fe/H] ≈ -0.5 dex (Walker 1993). We must remove the contamination by the young LMC field population before we

can proceed to analyze the color-magnitude diagram of Hodge 11. The maximum radial distance from the center of Hodge 11 for our WFPC2 observations is only $127.4''$. The core and tidal radii of Hodge 11 are $r_c = 18''$ and $r_t = 180''$, respectively (Mateo 1987). Our radial coverage of Hodge 11 is thus $0 \leq r \leq 7.1 r_c$ or $0 \leq r \leq 0.71 r_t$ and our observation is well within the tidal radius of the globular cluster. We are forced to *approximate* the LMC field population by erroneously assuming that *all* of the stars in the outer regions of our observation are LMC field stars. We split our observation into two regions: (1) the cluster region ($r \leq 83.2''$: 12281 stars — see Fig. 2b) and (2) the LMC field region ($r > 83.2''$: 894 stars — see Fig. 2c) which is comparable with the LMC field CMDs of Stryker *et al.* (1984: Fig. 1) and Walker (1993: Fig. 4).

We used the following procedure to statistically remove the LMC field population from the cluster region CMD. Every star in the cluster region CMD has a V magnitude with an error σ_V and a $B - V$ color with an error $\sigma_{(B-V)}$. For a given star in the cluster region CMD (Fig. 2b) we can count how many stars can be found in that CMD that have $B - V$ colors within $\mathrm{MAX}(2\sigma_{(B-V)}, 0.100)$ mag and V magnitudes within $\mathrm{MAX}(2\sigma_V, 0.200)$ mag. Let us call that number N_{H11}. We can also count how many stars can be found in the *field* region CMD (Fig. 2c) within the same V magnitude range and $B - V$ color range that was determined for the star in the *cluster* region CMD. Let us call that number N_{LMC}. The probability, p, that the star in the cluster region CMD is actually a cluster member of Hodge 11 can be approximated as follows

$$p \approx 1 - \mathrm{MIN}\left(\frac{\alpha(N_{\mathrm{LMC}} + 1)}{N_{\mathrm{H11}} + 1}, 1.0\right) \qquad (3)$$

where $\alpha \equiv 3.00$ which is the ratio of the area of the cluster region (3.58 arcmin^2) to the area of the LMC field region (1.19 arcmin^2). We see, by definition, that $N_{\mathrm{H11}} \geq 1$, $N_{\mathrm{LMC}} \geq 0$, and $0 \leq p \leq 1$. Now suppose for a given star in the cluster region CMD that we find $N_{\mathrm{H11}} = 78$ and $N_{\mathrm{LMC}} = 10$, then the probability of cluster membership is $p \approx 0.582$ or 58.2 percent. We can determine the probable cluster membership of this star by picking a uniform random number, $0 \leq p' \leq 1$, and if $p' \leq p$ then this star is said to probably be a cluster member. Using a uniform random number generator, we determined the probable cluster membership for all 12281 stars in the cluster region CMD field. Only 9506 stars were retained as probable cluster members and they are displayed as the cleaned cluster CMD (see Fig. 2d). Since the above CMD cleaning method is probabilistic, this figure represents only one out of an infinite number of different realizations of the cleaned Hodge 11 CMD. The cleaned Hodge 11 CMD diagram (Fig. 2d) contains 9506 stars which implies that about 23% of the stars in the cluster region CMD (Fig. 2b) are LMC field stars.

The cleaned cluster color-magnitude diagram (Fig. 2d) confirms previous findings that

Hodge 11 is a very metal-poor cluster with a steep red giant branch and a blue horizontal branch.

We confirm the finding of Walker (1993) that the distribution of horizontal branch stars in Hodge 11 is skewed to the extent that only blue HB stars appear. We find 124 blue HB stars, no RR Lyrae stars, and no red HB stars. Graham & Nemec (1984) and Walker (1993) have previously surveyed Hodge 11 for RR Lyrae stars but none were found.

We do not detect any significant gaps in the distribution of blue HB stars. This contradicts the finding of Walker (1993) that the blue HB stars in Hodge 11 are concentrated into two groups with a gap existing near $V \approx 19.6$ mag. Walker finds 43 blue HB stars whereas we find 124 and it is quite probable that the gap seen in Walker's Fig. 3 is simply due to counting statistics.

4. THE AGE OF HODGE 11

One of the most important goals of galactic astronomy is to understand how and when galaxies form and evolve. The oldest star clusters of the Magellanic Clouds preserve important information about the formation and evolution of these satellite galaxies of the Milky Way. Although an extensive literature exists on the properties of the Large and Small Magellanic Clouds, we know surprisingly little about their oldest stellar populations. This lack of knowledge about the formation epoch of the LMC and SMC, has greatly hampered our understanding of their physical and chemical evolution.

The ages of the oldest Large Magellanic Cloud star clusters are virtually unknown (Da Costa 1993). Besides Hodge 11, only five other LMC globular clusters have published CCD-based color-magnitude diagrams (NGC 1466: Walker 1992a; NGC 1841: Walker 1990; NGC 2210: Reid & Freedman 1994; NGC 2257: Walker 1989, Testa *et al.* 1995; Reticulum: Walker 1992b). Most of these CMDs were produced while investigating the RR Lyraes in these globular clusters. As a result, while they are all deep enough to determine the morphology of the horizontal branch, only one (NGC 2257: Testa *et al.* 1995) has photometry that reaches below the main-sequence turnoff.

Faced with the lack of accurate main-sequence photometry in the LMC globular clusters, researchers have used the horizontal-branch morphologies of these systems to study their ages relative to those of the Galactic halo globular clusters. Lee (1992) has shown that the HB morphology for fixed [Fe/H] varies with Galactocentric distance. Lee (1989) introduced the HB type index $(B - R)/(B + V + R)$ where B, R, and V, respectively, denote the number of blue HB stars, red HB stars, and RR Lyraes. The more distant clusters

tend to have redder HB types and the scatter of HB type at a given [Fe/H] increases with Galactocentric distance. This is indicative of the "second parameter" effect and is consistent with the halo formation model of Searle & Zinn (1978). Lee (1992) used his diagnostic [Fe/H] vs. $(B - R)/(B + V + R)$ diagram to compare 7 LMC and SMC globular clusters with Galactic globular clusters and found evidence that the LMC and SMC clusters formed about 2 Gyr after the formation of the inner Galactic halo globular clusters. Using the same technique, Walker (1992a) and Da Costa (1993) reached a similar conclusion that the age difference was 2–3 Gyr.

We find that the Lee HB morphology index for Hodge 11 is $1.00^{+0.00}_{-0.04}$ with 124 blue HB stars, 0 RR Lyraes, and 0 red HB stars. The lower limit is assumed to be due to counting statistics alone. The diagnostic [Fe/H] vs. $(B - R)/(B + V + R)$ diagram unfortunately becomes degenerate with very blue (or very red) horizontal branches, so Lee's HB index can not provide a useful estimate of the relative age difference between Hodge 11 and the Galactic halo globular clusters.

The robust mean $B - V$ color as a function of V magnitude of the Hodge 11 main-sequence and subgiant branch is listed in Table 3 and is shown graphically in Figs. 3 and 4. This fiducial sequence was derived using 0.2 mag bins and the robust mean color was determined after 3σ outliers were iteratively rejected. The reliability of this method can be checked in Fig. 3 by comparing the robust mean $B - V$ color (filled circles) with the median $B - V$ color (open diamonds) of all the stars in the same 0.2 mag bins. The median and robust-mean $B - V$ colors agree within the errors determined for the robust mean $B - V$ colors.

Spectroscopic abundance determinations by Cowley & Hartwick (1982) and Olszewski et al. (1991) agree that Hodge 11 is metal-poor with [Fe/H] $= -2.1 \pm 0.2$ dex. The steep red giant branch revealed in the color-magnitude diagrams of Stryker et al. (1984), Walker (1993), and our Figs. 2 and 4 are in complete agreement with the spectroscopic determination of the metallicity of Hodge 11.

We compare the Hodge 11 fiducial sequence with that of the metal-poor Galactic globular cluster M92 (Stetson & Harris 1988) in Figs. 3 and 4. We find that by making the M92 fiducial sequence fainter by $\Delta V = 4.05$ mag and adding an additional reddening of $\Delta(B - V) = 0.055$ mag gives an excellent fit to the Hodge 11 fiducial sequence. The upper and lower limits of these shifts, as shown in Fig. 3, are $\Delta V = 4.05 \pm 0.05$ mag and $\Delta(B - V) = 0.055 \mp 0.010$ mag.

Stetson & Harris (1988) found that the apparent distance modulus of M92 is $(m - M)_V \approx 14.6$ mag and adopted the reddening of E$(B - V) = 0.02$ mag. The reddening

of Hodge 11 is thus $\mathrm{E}(B-V)_{\mathrm{H11}} \approx \mathrm{E}(B-V)_{\mathrm{M92}} + \Delta(B-V) \approx 0.075 \pm 0.005$ mag which is in excellent agreement with Walker's (1993) estimate of $\mathrm{E}(B-V) = 0.08 \pm 0.02$ mag. The apparent distance modulus of Hodge 11 is $(m-M)_{V,\mathrm{H11}} \approx (m-M)_{V,\mathrm{M92}} + \Delta V \approx 18.65 \pm 0.12$ mag where we have assumed an error of 0.10 mag for $(m-M)_{V,\mathrm{M92}}$. The true distance modulus of Hodge 11 is then $(m-M)_o \approx 18.42 \pm 0.12$ mag assuming that $A_V = 3.1\mathrm{E}(B-V) \approx 0.23 \pm 0.02$ mag (Savage & Mathis 1979).

Hodge 11 is $4\overset{\circ}{.}71$ (Mateo 1987) from the rotation center of the LMC given by Rohlfs *et al.* (1984). Walker (1993) notes that if it is assumed that Hodge 11 lies in the LMC disk then the inclination correction for the distance modulus is 0.09 mag in the sense that Hodge 11 is closer to us than the LMC center. If we add this inclination correction to our determination of the distance modulus of Hodge 11 we then derive a distance modulus for the LMC of $(m-M)_o = 18.51 \pm 0.17$ mag which is in excellent agreement to the value 18.5 mag of Westerlund (1990) and van den Bergh (1991). For comparison, Crotts, Kunkel, & Heathcote (1995) find the distance modulus of the LMC to be 18.57 ± 0.13 mag based on light travel time measurements across the ring of SN 1987A.

We can determine the relative age difference between M92 and Hodge 11 in the following manner. We estimate the absolute visual magnitude of the main-sequence turnoff of Hodge 11 to be $V_{\mathrm{TO,H11}} \approx 22.65 \pm 0.10$ mag. The absolute visual magnitude of the main-sequence turnoff of Hodge 11 is then $M_{V,\mathrm{H11}}^{\mathrm{TO}} \approx 4.00 \pm 0.16$ mag. The absolute visual magnitude of the main-sequence turnoff of M92 is $M_{V,\mathrm{M92}}^{\mathrm{TO}} \approx 4.00 \pm 0.14$ mag assuming $V_{\mathrm{TO,M92}} = 18.60 \pm 0.10$ mag (Stetson & Harris 1988). The *difference* between these turnoffs is $M_{V,\mathrm{H11}}^{\mathrm{TO}} - M_{V,\mathrm{M92}}^{\mathrm{TO}} = 0.00 \pm 0.21$ mag which gives an age resolution of $\sim$21% using Eq. 2 of Mighell & Butcher (1992). We have thus found that $age_{\mathrm{H11}}/age_{\mathrm{M92}} \approx 1.00 \pm 0.21$ which translates to $age_{\mathrm{H11}} \approx 15 \pm 3$ Gyr if M92 is assumed to be 15 Gyr old. This is probably a conservative estimate of the true relative age-difference uncertainty between M92 and Hodge 11. If we naively assume that the only source of uncertainty is our error in determining $V_{\mathrm{TO,H11}}$ and the V magnitude shift between the M92 and Hodge 11 fiducial sequences then we find that $M_{V,\mathrm{H11}}^{\mathrm{TO}} - M_{V,\mathrm{M92}}^{\mathrm{TO}} = 0.00 \pm 0.11$ mag which gives an optimistic age resolution of $\sim$10% using Eq. 2 of Mighell & Butcher (1992). The relative age-difference uncertainty between Hodge 11 and M92 is probably between 10 and 21 percent.

Our analysis suggests that, within the accuracy of our photometry, Hodge 11 is as old as M92 — probably one of the oldest globular clusters in the Milky Way. Furthermore, if we assume that the globular cluster Hodge 11 has always been a part of the Large Magellanic Cloud and was not stripped from the halo of the Milky Way or absorbed from a cannibalized dwarf spheroidal galaxy, then the oldest stars in the Large Magellanic Clouds and the Milky Way appear to have the same age.

REFERENCES

Buonanno, R., Corsi, E., & Fusi Pecci, F. 1985, A&A, 145, 97

Burrows, C. J. 1994, Wide Field and Planetary Camera 2 Instrument Handbook, edited by C. J. Burrows, STScI publication (May 1994)

Cowley, A., & Hartwick, F. D. A. 1982, ApJ, 259, 89

Crotts, A. P. S., Kunkel, W. E., & Heathcote, S. R. 1995, ApJ, 438, 724

Da Costa, G. S. 1993, in The Globular Cluster-Galaxy Connection, ASP Conference Series, Vol. 48, G. H. Smith and J. P. Brodie (eds.)

Elson, R. A. W., & Fall, S. M. 1988, AJ, 96, 1383

Gascoigne, S. C. B. 1966, MNRAS, 134, 59

Girardi, L., Chiosi, C., Bertelli, G., & Bressan, A. 1995, A&A, 298, 87

Graham, J. A., & Nemec, J. M. 1984, in Structure and Evolution of the Magellanic Clouds, IAU Symposium No. 108, edited by S. van den Bergh and K. S. de Boer (Reidel, Dordrecht), p. 37

Hodge, P. W. 1960, ApJ, 131, 351

Holtzman, J. A., Hester, J. J., Casertano, S., Trauger, J. T., Watson, A. J., Ballester, G. E., Burrows, C. J., Clarke, J. T., Crisp, D., Evans, R. W., Gallagher J. S., Griffiths, R. E., Hoessel, J. G., Matthews, L. D., Mould, J. R., Scowen, P. A., Stapelfeldt, K. R., & Westphal, J. A. 1995a, PASP, 107, 156

Holtzman, J. A., Burrows, C. J., Casertano, S. Hester, J. J., Trauger, J. T., Watson, A. M., & Worthey, G. S. 1995b, PASP, 107, 1065

Krist, J. 1993, in Astronomical Data Analysis Software and Systems II, ASP Conf. Ser. Vol. 52, edited by R. J. Hanisch, R. J. V. Brissenden, and J. Barnes., p. 530

Krist, J. 1994, Tiny Tim User's Manual Version 4.0 (July 8, 1994)

Lee, Y.-W. 1989, Ph.D. thesis, Yale University

Lee, Y.-W. 1992, PASP, 104, 798

Mateo, M. 1987, ApJ, 323, L41

Mighell, K. J., & Butcher, H. R. 1992, A&A, 255, 26

Mighell, K. J., & Rich, R. M. 1995, AJ, 110, 1649

Mighell, K. J., & Rich, R. M. 1996, AJ (in press)

Rich, R. M., & Mighell, K. J. 1995, ApJ, 439, 145)

Olszewski, E. W., Schommer, R. A., Suntzeff, N. B., & Harris, H. C. 1991, AJ, 101, 515

Rohlfs, K., Kreitschmann, J., Siegmann, B. C., & Feitzinger, J. V. 1984, A&A, 137, 343

Savage, B. D., & Mathis, J. S. 1979, ARA&A, 17, 73

Searle, L., Wilkinson, A., & Bagnuolo W. G. 1980, ApJ, 239, 803

Searle, L., and Zinn, R. J. 1978, ApJ, 225, 357

Stetson, P. 1987, PASP, 99, 191

Stetson, P., & Harris, W. E. 1988, AJ, 96, 909

Stryker, L. L., Nemec, J. M., Hesser, J. E., & McClure, R. D. 1984, in Structure and Evolution of the Magellanic Clouds, IAU Symposium No. 108, edited by S. van den Bergh and K. S. de Boer (Reidel, Dordrecht), p. 43

Testa, V., Ferraro, F. R., Brocato, E., & Castellani, V. 1995, MNRAS, 275, 454

van den Bergh, S. 1991, ApJ, 369, 1991

Walker, A. R. 1989, AJ, 98, 2086

Walker, A. R. 1990, AJ, 100, 1532

Walker, A. R. 1992a, AJ, 104, 1395

Walker, A. R. 1992b, AJ, 103, 1166

Walker, A. R. 1993, AJ, 106, 999

Westerlund, B. E. 1990, A&ARev, 2, 29

– 13 –

FIGURE CAPTIONS

Fig. 1.— Comparison of our photometry with Walker (1993). We have 80 stars in common on the WF4 CCD of the WFPC2 instrument. A robust estimate of the mean difference in V (using 2σ rejection of outliers) is 0.009 ± 0.010 mag with our V magnitudes being $\sim 1\%$ fainter. This V zeropoint difference is not statistically significant. The seeing varied from 1.5 to 2.0 arcsec when Walker (1993) observed Hodge 11. Almost all of the stars with large V magnitude differences contain more than one star within a circular aperture of radius 1.0 arcsec (10 pixels) on the WF4 CCD.

Fig. 2.— The V vs $B - V$ color-magnitude diagram of the observed stellar field in the LMC globular cluster Hodge 11. The *Hubble Space Telescope* WFPC2 instrument was used to make one 300-s observation with the F555W filter and one 600-s observation with the F450W filter. (a) The 13175 stars are plotted with filled circles and the 1855 CCD defects are plotted with open circles. The CCD defects were identified using the procedure described in the text. (b) The 12281 stars within $83.2''$of the center of the globular cluster are plotted. (c) The 894 stars beyond $83.2''$of the center of the globular cluster are plotted. (d) The "cleaned" color-magnitude diagram of Hodge 11 with 9506 stars. The details of the statistical field-subtraction are described in the text.

Fig. 3.— The fiducial sequence of Hodge 11 (filled circles) compared with the M92 fiducial sequence of Stetson & Harris (1988). The M92 fiducial sequence is shown from left to right assuming a shift in $B - V$ color of 0.045, 0.055, and 0.065 mag and a shift in V magnitude of 4.10, 4.05, and 4.00 mag, respectively. The fiducial sequence of Hodge 11 was derived using 0.2 mag bins and the robust mean color was determined after 3σ outliers were iteratively rejected. The reliability of this method is checked by comparing the robust mean $B - V$ color (filled circles) with the median $B - V$ color (open diamonds) of all the stars in the same 0.2 mag bins.

Fig. 4.— The "cleaned" V vs $B - V$ color-magnitude diagram of LMC globular cluster Hodge 11 compared with M92 fiducial sequences. The Hodge 11 fiducial sequence is plotted with open circles. The lower curve is the M92 fiducial sequence of Stetson & Harris (1988). The solid curves on the left and at the top are, respectively, the fiducial sequences of the M92 horizontal branch and the M92 asymptotic giant branch of Buonanno, Corsi, & Fusi Pecci (1985). All M92 fiducial sequences are shown assuming $\Delta(B - V) = 0.055$ mag and $\Delta V = 4.05$ mag.
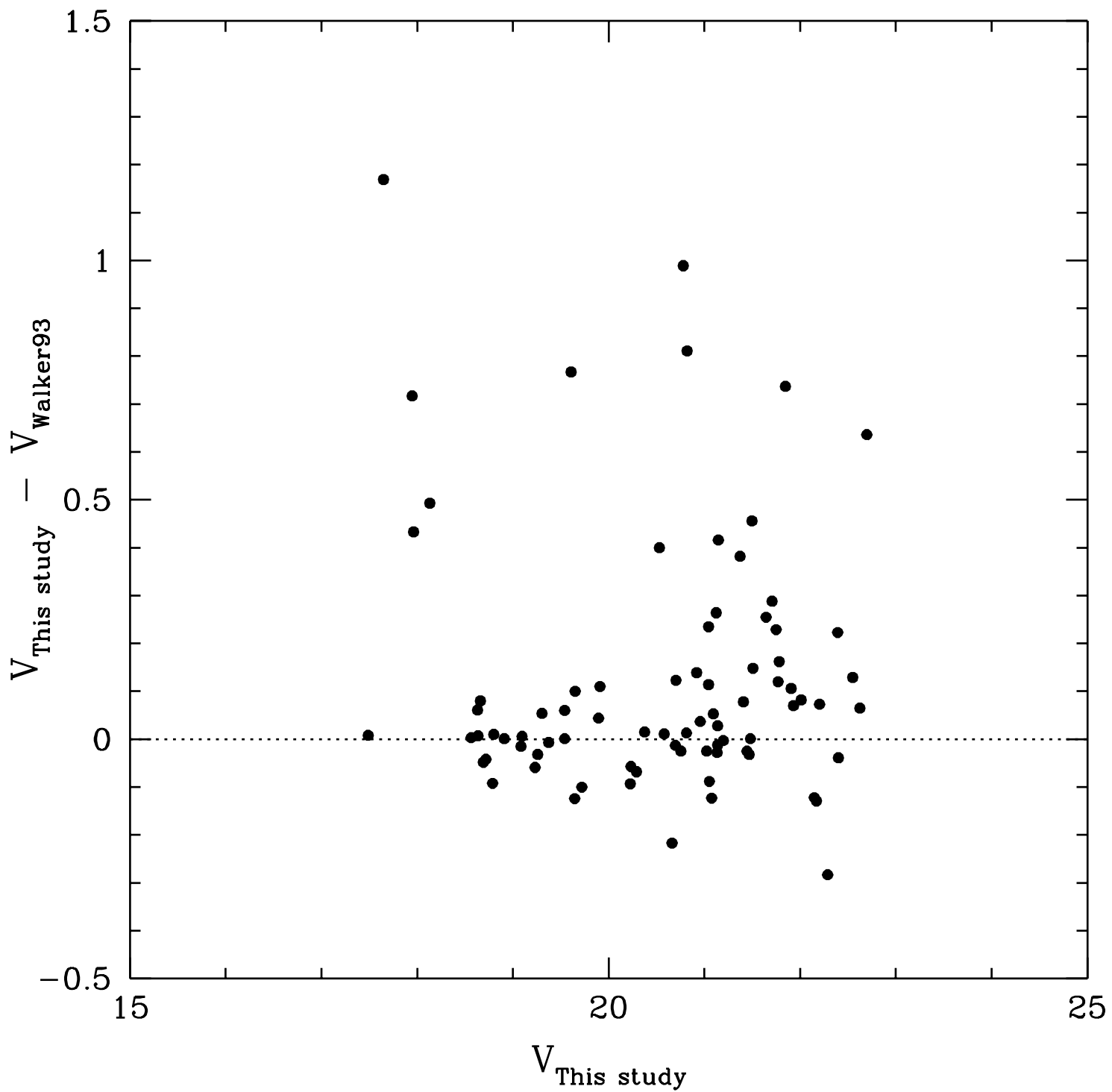
Figure 1 of Mighell, Rich, Shara, & Fall (1996)

TABLE 1. Calibration reference files.

KEYWORD	dataset	comment
MASKFILE	F8213081U.R0H	Input DQF of known bad pixels
ATODFILE	DBU1405FU.R1H	A-to-D conversion file
BIASFILE	E4P16298U.R2H	bias frame reference file
BIASDFIL	E4P16298U.B2H	bias frame reference DQF
DARKFILE	E1Q14338U.R3H	dark reference file
DARKDFIL	E1Q14338U.B3H	dark reference DQF
FLATFILE	E380934NU.R4H	F450W flat field reference file
FLATDFIL	E380934NU.B4H	F450W flat field reference DQF
FLATFILE	E380935CU.R4H	F555W flat field reference file
FLATDFIL	E380935CU.B4H	F555W flat field reference DQF
GRAPHTAB	E8210190M.TMG	HST graph table
COMPTAB	DC61424RM.TMC	HST components table

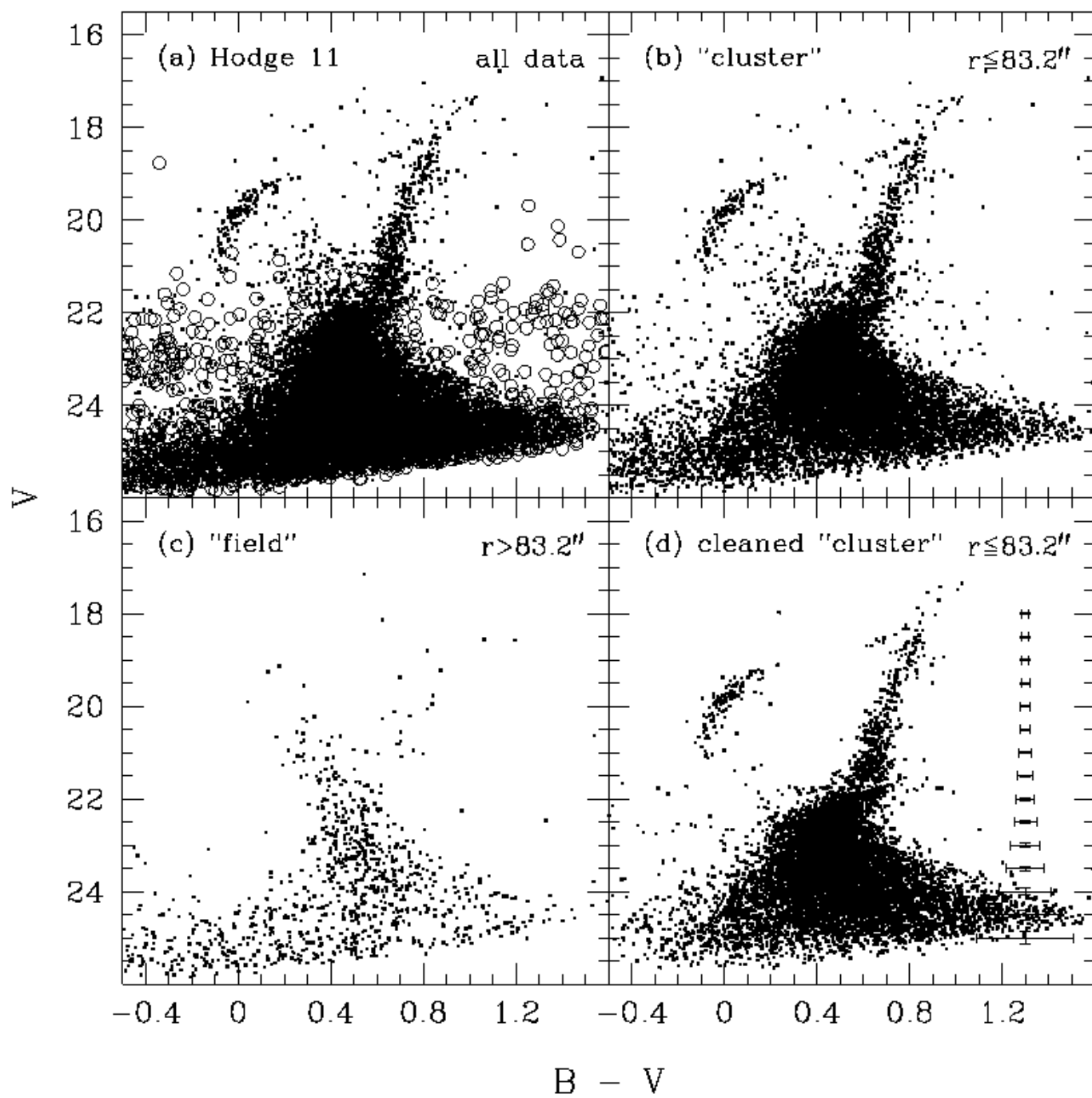Table 1 of Mighell, Rich, Shara, & Fall (1996)

Figure 2 of Mighell, Rich, Shara, & Fall (1996)

TABLE 2. Aperture corrections.

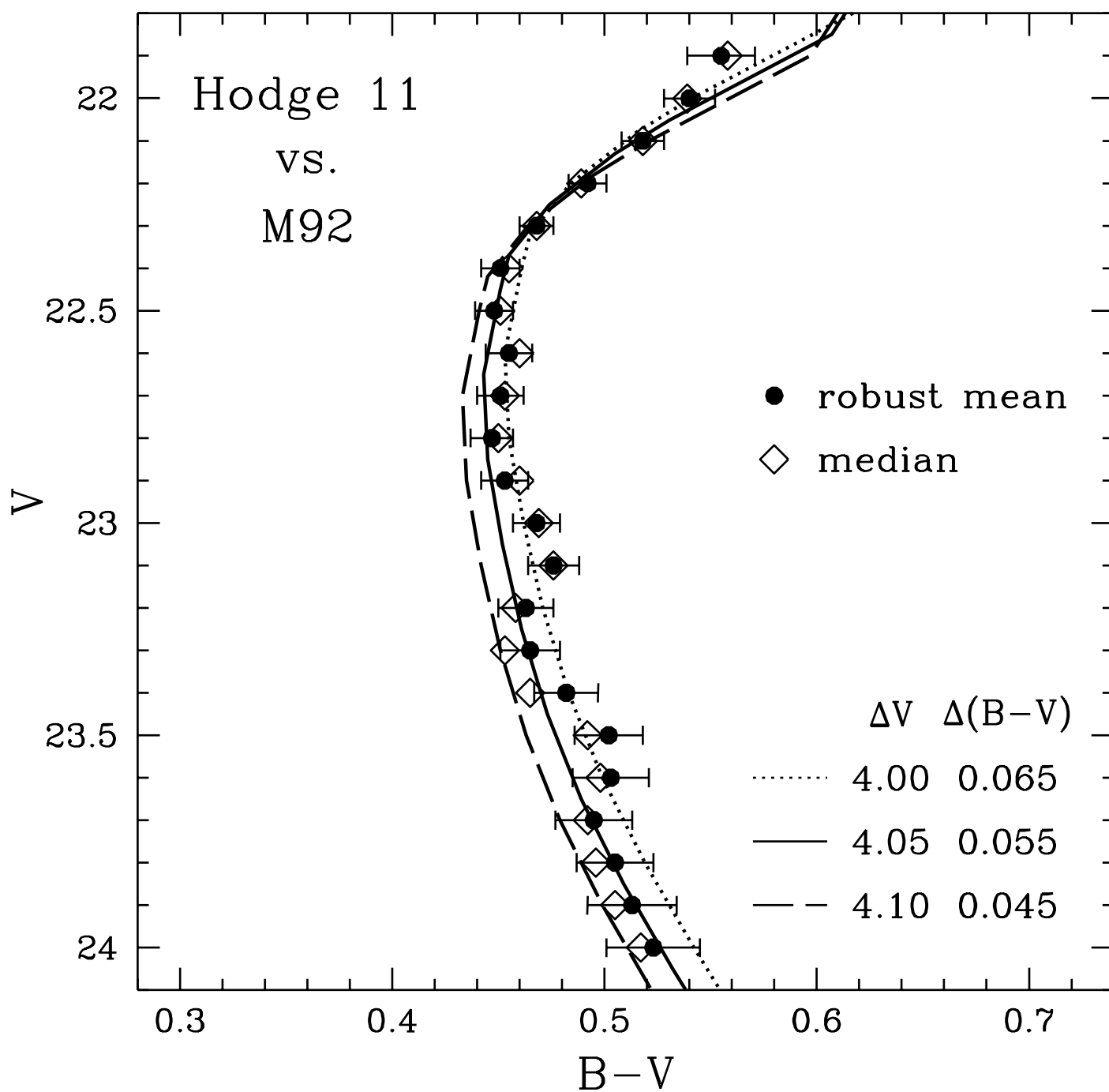| Filter	CCD	$\overline{\Delta m_r}$ [mag]	Δm_0 [mag]	Δm_∞ [mag]
F450W	PC1	-0.506±0.021	0.045	0.093
F450W	WF2	-0.307±0.012	0.055	0.102
F450W	WF3	-0.378±0.025	0.113	0.107
F450W	WF4	-0.331±0.011	0.062	0.105
F555W	PC1	-0.568±0.021	0.066	0.095
F555W	WF2	-0.320±0.013	0.069	0.102
F555W	WF3	-0.389±0.023	0.107	0.106
F555W	WF4	-0.343±0.011	0.069	0.104

Table 2 of Mighell, Rich, Shara, & Fall (1996)

Figure 3 of Mighell, Rich, Shara, & Fall (1996)

TABLE 3. The Hodge 11 fiducial sequence.

| V [mag]	$B-V$ [mag]	$\sigma_{(B-V)}$ [mag]	n
21.9	0.555	0.016	145
22.0	0.540	0.012	152
22.1	0.518	0.010	182
22.2	0.492	0.009	262
22.3	0.468	0.008	309
22.4	0.451	0.009	343
22.5	0.448	0.009	387
22.6	0.455	0.011	444
22.7	0.451	0.011	472
22.8	0.447	0.010	508
22.9	0.453	0.011	526
23.0	0.468	0.011	526
23.1	0.476	0.012	575
23.2	0.463	0.013	593
23.3	0.465	0.014	608
23.4	0.482	0.015	653
23.5	0.502	0.016	706
23.6	0.503	0.018	740
23.7	0.495	0.018	720
23.8	0.505	0.018	724
23.9	0.513	0.021	774
24.0	0.523	0.022	781

Table 3 of Mighell, Rich, Shara, & Fall (1996)
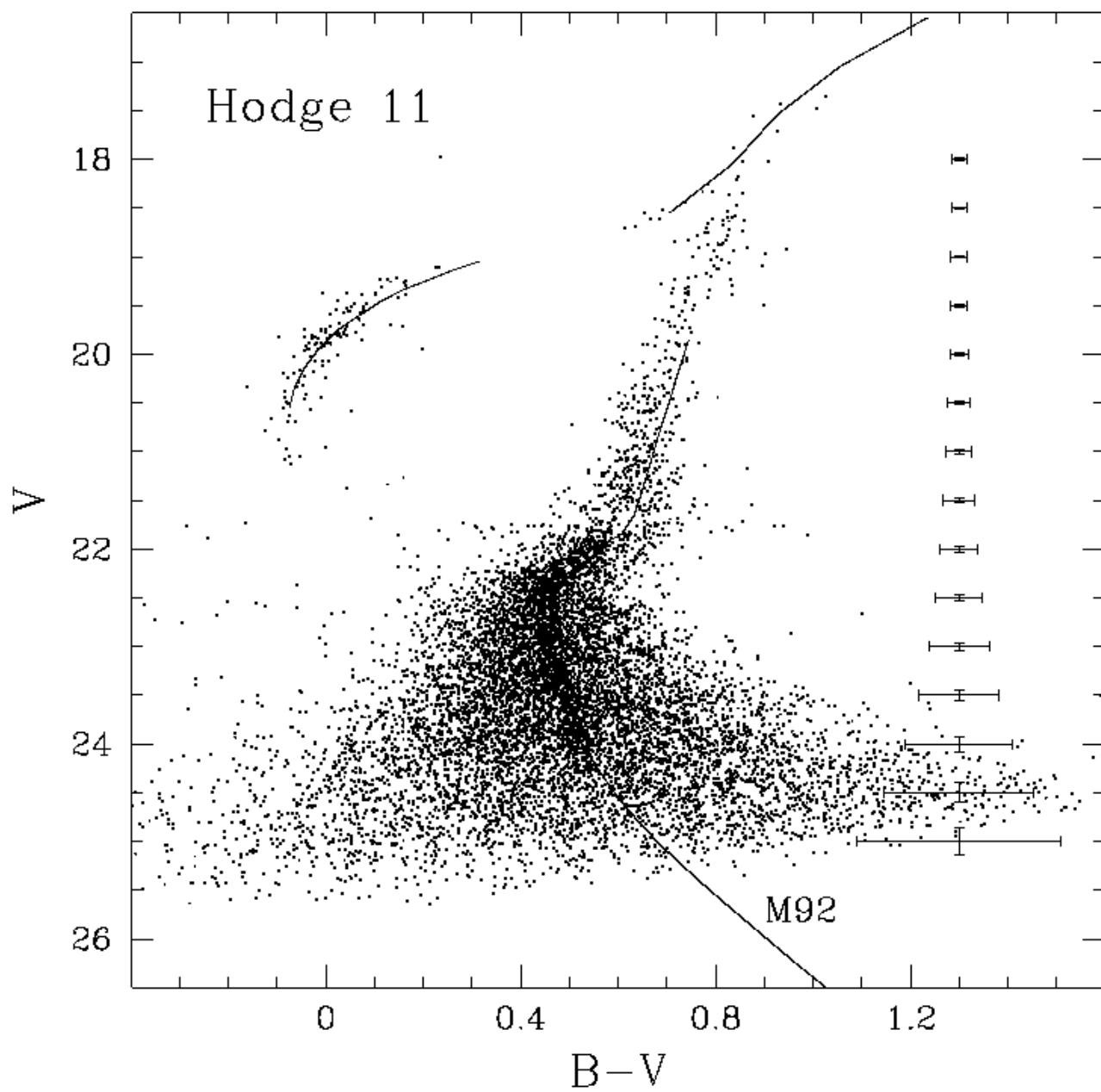
Figure 4 of Mighell, Rich, Shara, & Fall (1996)